Assessing Salt-Surfactant Synergistic effects on Interfacial Tension from Molecular Dynamics Simulations

Gerard Alonso [a], Pablo Gamallo [a], Andrés Mejía [b], Ramón Sayós [a,*]

[a] *Departament de Ciència de Materials i Química Física & Institut de Química Teòrica i Computacional (IQTCUB), Universitat de Barcelona, C. Martí i Franquès 1, 08028 Barcelona, Spain.*

[b] *Departamento de Ingeniería Química, Universidad de Concepción, POB 160-C, Correo 3, Concepción, Chile.*

Abstract: In the recent years, many efforts have been carried out trying to comprehend how surfactants and salts interact among each other at the oil/brine interface to reduce the interfacial tension (IFT). To that end, the interfacial properties of several combinations of surfactants, salts and oils have been measured experimentally confirming the existence of a synergistic effect. Unfortunately, many of the proposed mechanisms for that effect arise from experimental observations, so this work, based on molecular dynamics simulations, intends to reproduce and explain this kind of phenomenon from a molecular point of view. The correct understanding of these phenomena can have application in many fields, especially in Enhanced Oil Recovery, where reducing IFT can potentially increase oil production. In this article we evaluate the effect of adding three different salts (i.e., NaCl, $CaCl_2$ and $MgCl_2$) on the IFT of a water/oil system with different non-ionic surfactants. We have evaluated the effect that the ions of salt produce to surfactants, as well as the perturbation that surfactants produce on the ions. From our results, we can assess that salts (especially NaCl) and surfactants are able to interact with each other, being both active species in reducing the IFT of the system.

Keywords: Molecular Dynamics simulations, Interfacial tension, Oil/water interface, Surfactant, Salt, Synergistic effect

Corresponding Author

*E-mail adress: r.sayos@ub.edu (Ramón Sayós)

1. Introduction

The use of surfactants in Enhanced Oil Recovery (EOR) is a common practice to reduce the interfacial tension (IFT) between crude oil and formation water [1–3]. The IFT reduction enhances the mobility of the crude oil within the reservoir, weakening the capillary forces, and ultimately improving oil production. The application of these compounds is usually expensive, so many studies have been focused on replacing them with other cheaper compounds. A good example is the low-salinity waterflooding, which permitted to enhance oil recovery by only controlling the salinity of the injection water in certain reservoirs [4, 5]. However, the best performance is usually obtained with a combination of surfactants and other additives (e.g, co-surfactants) to the oil/water/surfactant mixture [6–8]. Both compounds can act cooperatively to reduce the IFT to ultralow values and can improve the stability of oil/water microemulsions [9]. Also, similar synergistic interactions were observed experimentally when using salts as additives [10–23].

Species with highly localized charge, such as ions of salts, are capable of interacting with polar molecules and polar functional groups, changing their microscopical ordering and affecting their physicochemical properties. For example, water molecules orient their dipoles towards ions in solution forming highly order solvation shells due to strong electrostatic interactions. This fact affects the water density, viscosity, surface tension, melting point, boiling point and vapor pressure [24–26]. Similarly, the ions of salts can modify the surfactant solubility in water, its Critical Micelle Concentration (CMC) [27–29] or the IFT of liquid/liquid and vapor/liquid systems. In particular, the equilibrium IFT (i.e., usually called static IFT) of several water/surfactant + salt mixtures was studied by different authors, showing reductions of the IFT based on the so-called salt-surfactant synergistic effect. Some examples are the works of Staszak et al. [22], who studied a water/zwitterionic surfactant/NaCl system, Koelsch et al. [18], who analyzed different water/cationic surfactant/potassium halide salt systems or Fainerman et al. [14], who reported results for different water/anionic surfactant/NaCl+$CaCl_2$+$MgCl_2$ systems, among others [11–13, 15, 16]. Finally, these synergistic effects were mainly seen at surfactant concentrations below the CMC [18, 22, 23]. Notice that the static IFT value is achieved after waiting for all species to diffuse to their equilibrium positions. During this

process, which can take several minutes or hours, the IFT is not constant. The variation of the IFT with time is called dynamic IFT and it converges smoothly to the static IFT. However, this property is also affected by the salt-surfactant synergistic effect, changing the dynamic IFT pattern to an abrupt decrease to an IFT minimum (i.e., sometimes even drops to ultralow values) followed by a smooth increase until it converges with the static IFT. This behavior was reported by authors such as Liu et al. [20,21], who studied the dynamic IFT of different water/anionic + non-ionic surfactants/salt systems or Witthayapanyanon et al. [23], who performed measurements in mixtures containing water/anionic surfactant/NaCl.

The aforementioned experimental evidence served to propose different mechanisms to explain both the static and the dynamic IFT reduction phenomena. Two mechanisms were proposed to explain the static IFT reduction: (i) salinity reduces the solubility of surfactants in water, which forces them to migrate to the interface [30]; (ii) the salt ions can interact with the surfactant head groups and minimize the electrostatic interaction among them, which induces a closer packing of surfactants at the interface to allow additional surfactant molecules to fit at the interface [20, 21]. Alternatively, the dynamic IFT reduction mechanism proposed assumes that surfactants are soluble in both the oil and the water phase. Then, the solubility of surfactants in water is lessened upon addition of salts, which promotes the diffusion of surfactants from the water to the oil phase through the oil/water interface. The minimum in the dynamic IFT is assumed to occur when the surfactant molecules that are diffusing to the oil phase, are close to the interface [31]. Finally, the IFT is increased again when they are at equilibrium in the oil bulk. In summary, all previous mechanisms were mainly deduced from experimental measurements, who relate the IFT reduction with an increased number of surfactants at the interface, based on the Gibbs adsorption isotherm [32]:

$$d\gamma = -\sum_i \Gamma_i \, \mu_i \tag{1}$$

where γ is the IFT of the system and μ_i and Γ_i are the chemical potential and the interfacial excess concentration of species i at the interface for a given temperature. The ideal interface, represented by the Gibbs absorption isotherm, has an infinitesimal volume and is placed at the Gibbs dividing surface (σ). For convenience, one should place σ at the position that makes the Γ_i of a reference component (e.g., water) equal to zero and refer

other Γ_i to that component (i.e., Γ_i^w for water as reference). Finally, Eq. (1) can be rearranged as:

$$\Gamma_i^w = -\frac{1}{RT}\left(\frac{\partial \gamma}{\partial \ln(a_i)}\right)_{T,a_{j\neq i}} \quad (2)$$

Notice that for diluted concentrations the activity a_i in Eq. (2) can be taken simply as the concentration. The expression indicates that the interfacial excess of a species *i* can be either negative or positive as a function of the interfacial behavior of this compound. If this compound accumulates at the interface the value of Γ_i^w is positive and the IFT is reduced upon addition of this compound to the solution. These types of species are known as surface active compounds. On the other hand, if a compound depletes from the interface the value of Γ_i^w becomes negative and the IFT is increased upon addition of this compound.

The need of better understanding the interactions between salts and surfactants, motivated some simulation studies that combined ionic surfactants and salts [33–35]. From these works, it was observed that anionic surfactants, which have negatively charged head groups and usually Na^+ counterions, are capable of exchanging their Na^+ by divalent cations of the salt. This exchange is favored because divalent cations have more charge and interact more strongly with the charged head groups than Na^+. Similarly, cationic surfactants, which have positively charged head groups and are commonly accompanied by Cl^- counterions, are capable of exchanging their Cl^- by divalent anions of the salt. Their main conclusion was that these ionic exchanges modify the electrostatic interactions at the interface, which perturb the interfacial molecular distributions. However, none these works characterized the IFT reduction phenomena due to salt-surfactant synergistic effects via molecular simulations.

To expand the knowledge in salt-surfactant interfacial phenomena, Molecular Dynamics (MD) simulations on oil/water/surfactant/salt systems are performed, using pure dodecane as model oil, three different chlorine salts (i.e., NaCl, $CaCl_2$ or $MgCl_2$) and two non-ionic surfactants: the Triethyleneglycol 1-dodecyl ether (i.e., $CH_3(CH_2)_{11}(OCH_2CH_2)_3OH$ also known as $C_{12}E_3$), which is a linear surfactant with 12 CH_x tail groups and a head with three polyoxyethylene units and an alcohol termination, and triethyleneglycol 6-dodecyl ether (i.e., $(CH_3(CH_2)_5)(CH_3(CH_2)_4)CH(OCH_2CH_2)_3OH$ alternatively named $(C_6C_5)CE_3$). The latter is a version of the same surfactant but with a

ramified tail. Thus $(C_6C_5)CE_3$ and $C_{12}E_3$ share the same head group, and both tail groups have the same molecular weight for the sake of evaluating the effect of the ramification in the tail group. The purpose of these simulations is to explain the experimental trends in the static IFT reduction and give an alternative perspective to this phenomenon from a molecular point of view. Due to the MD simulations yielding equilibrium properties, only salt-surfactant synergistic effects on the static IFT are evaluated, while the dynamic IFT processes are not taken into account.

Although the correct characterization of the static salt-surfactant synergistic effect has a significant impact in EOR (i.e., helping to lower the IFT and thus increasing production), it is only one of the many phenomena involved in the complex process of oil recovery. In fact, the presence of salts can also activate other mechanisms that hamper the oil extraction. For example, it is well known that depending on the rock matrix, salt cations can attach to the mineral surface and attract the negatively charged polar fraction of crude oils to the rock, which ultimately reduce the wettability of the reservoir [36]. In that situation, the effectivity of the recovery would be conditioned by the balance between all the mechanisms activated in presence of salinity. This means that unless the static salt-surfactant synergistic effect is capable defeating all other processes (i.e., by significantly reducing the IFT) it might not be directly applicable to EOR. In any case, this effect is present in any oil recovery process, so understanding it can help to unveil some of the mechanisms occurring during oil recovery.

2. Computational methods

MD simulations with classical force fields were performed by means of LAMMPS code [37]. The initial simulation cell to calculate IFT consists on an orthorhombic box with dimensions $L_x = L_y = 80$ Å and $L_z = 210$ Å. Half of the simulation cell was filled with water molecules at $\rho = 0.997$ g/cm^3 and the other half was filled with dodecane at $\rho = 0.745$ g/cm^3. Both values correspond to the experimental pure liquid densities at $T = 300$ K and $P = 1$ atm [38,39]. The three different salts (i.e., NaCl, $CaCl_2$ or $MgCl_2$) were inserted only in the water phase at a 2.0 molal concentration. Notice that this concentration is significantly higher than the average seawater salinity (i.e.,~0.6 M) typically used in waterflooding, or the optimum salinities commonly employed in low-salinity/surfactant EOR. In fact, low-salinity is favored during oil recovery because it helps surfactants to achieve ultralow dynamic IFT, and the wettability of the rocks is increased in absence of salinity. However, in the present work, equilibrium MD simulations of the liquid/liquid interface were conducted, where neither the dynamic effects or the interactions with the rock are taken into consideration. Regarding static IFT reductions, some experimental works seemed to show stronger effects at higher salinity concentrations up to 2.0 M [16, 20–22]. For this reason, three preliminary calculations were carried out to find the salinity concentration that maximized the static IFT reduction effect in the considered oil/water/surfactant systems: (i) no significant change on the equilibrium IFT was observed at 0.5 molal of NaCl, (ii) a statistically meaningful reduction effect was detected at 2.0 molal of NaCl and (iii) the IFT was increased when calculated at 6.0 molal of NaCl. Finally, the surfactants were added directly onto the water/oil interface to accelerate the equilibration of the system at a concentration below the CMC. The amount of surfactants simulated represents an interface with an interfacial excess $\Gamma_i^w = 1.50$ μmol/m^2 (i.e., 110 Å^2/molecule) and it has been chosen in consistency with the aforementioned experiments performed (i.e., below the CMC) [11–13, 15, 16, 18, 22, 23]. The initial position and orientation of all molecules followed a uniform random distribution with the only restriction that molecules can only be generated in the respective regions detailed. Fig. 1 shows a typical simulation cell with a summary of all species involved in our simulations.

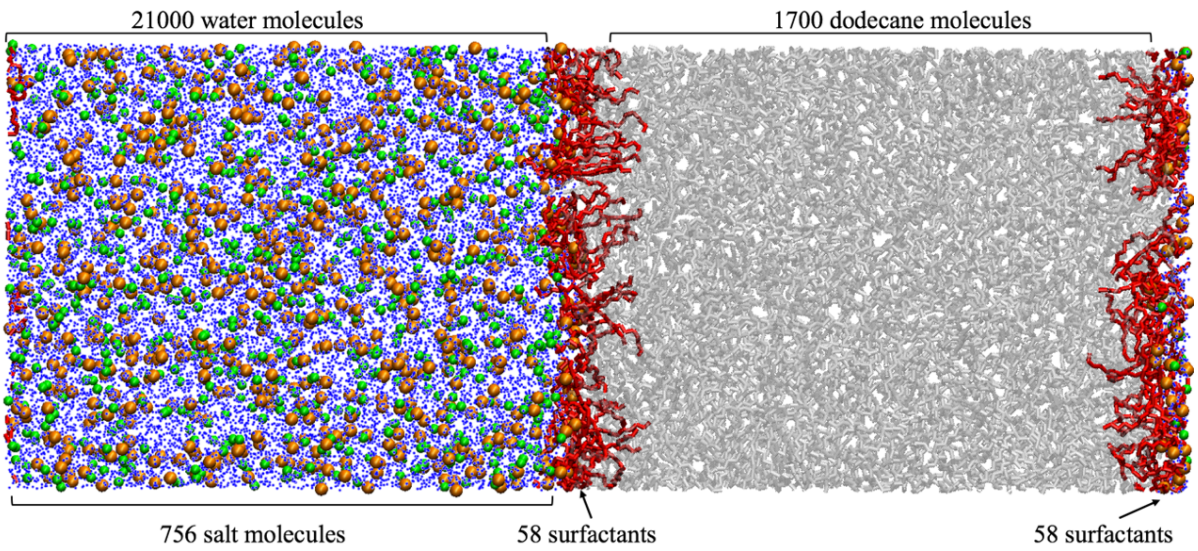

Fig 1. Summary of molecules used in the standard 80 Å x 80 Å x 210 Å simulation cell with two interfaces. Dodecane and water molecules are represented by grey bonds and blue dots, respectively. Ionic salts are represented by spheres: the cation in orange and the anion in green. Finally, the surfactant molecules are displayed in red bonds accumulated at the interface.

177

178 The simulations were performed in three steps: first, the random creation of particles
179 required an initial minimization of the system to avoid molecular overlaps. Second, the
180 system was thermalized in the NVT ensemble, using first a Langevin thermostat [40]
181 during 20 ps followed by 100 ps with a Nosé-Hoover thermostat [41], a combination of
182 thermostats that was very efficient for thermal equilibration. Third, a Berendsen barostat
183 [42] was used to equilibrate the pressure during 500 ps, while temperature was still
184 controlled by the Nosé-Hoover thermostat. The barostat only couples to the z-direction
185 of the simulation cell to keep interfacial area constant (i.e., NAP_ZT ensemble). Finally,
186 the Berendsen barostat was changed by a Nosé-Hoover barostat [43] to perform a time
187 evolution of 20 ns. The thermostat and barostat constants were 0.2 and 1.0 ps respectively
188 and the timestep for all simulation stages was 1 fs.

189 Block averages were extracted each 0.5 ns to monitor the evolution of the total energy
190 and interfacial tension of the system. In most simulations the equilibrium was reached
191 after 10 ns of evolution, and the range from 10 to 20 ns was used to calculate the
192 equilibrium IFT. For those calculations with longer equilibration times, 10 extra ns were
193 run to calculate the averages from this additional time. Also, to ensure that calculations
194 were fully converged, a single calculation was time evolved during 50 extra ns, obtaining
195 an equivalent value of IFT compared to the one calculated up to 20 ns. Finally, the
196 molecular distributions were calculated using the final 2 ns of the simulation. Notice that

197 the large interfacial area (i.e., 80 Å x 80 Å) employed in the simulations improve the
198 statistical significance of the molecular distributions. This means that averaging 2 ns is
199 enough to yield smooth density profiles as shown in the results section.

200 Intermolecular and intramolecular interactions of organic molecules were represented
201 with the TraPPE-UA force field [44]. This force field considers that bonds are fixed at
202 their equilibrium bond lengths, so we followed the standard recommendation of TraPPE
203 developers and used the spring constants from AMBER force field [45] to allow
204 molecular vibrations. Water molecules were reproduced using the rigid TIP3P force field
205 [46], which were constrained to their equilibrium geometry through the SHAKE
206 algorithm [47]. A validation stage of TraPPE-UA and TIP3P force fields was carried out
207 to ensure that the models were correctly reproducing the properties of the surfactants and
208 water. The validation is compiled in the Supplementary Material, where it is seen that the
209 surfactants are well reproduced by TraPPE-UA. Similarly, the salt-surfactant synergistic
210 effects identified in this work can also be seen with more sophisticated water models such
211 as TIP4P/Ew [48]. However, the TIP4P model of water is computationally more
212 expensive than a standard three-point model such as TIP3P. So, after ensuring that the
213 latter is capable of capturing the salt-surfactant synergistic effect (see section S1 of the
214 Supplementary Material), it is selected due to computational efficiency. Finally, the ions
215 of salts (i.e., Na^+, Ca^{2+}, Mg^{2+}, Cl^-) are compounds hard to simulate by point charge
216 models, as can be seen by the large amount of force fields developed by many authors on
217 the last years. To evaluate the effect of the force field on the calculated properties,
218 simulations with salts were performed with three different non-polarizable sets of
219 parameters: (i) the force field from Smith and Dang [49], whose parameters are
220 implemented in CLAYFF; (ii) the force field from Åqvist [50], used in OPLS; and (iii)
221 the force field from Beglov and Roux [51], found in the CHARMM force field. Crossed
222 interactions between all species in this work are accounted through the standard Lorentz-
223 Bethelot mixing rules [52]. All pair interactions were calculated using a spherical cutoff
224 of 14 Å as recommended by TraPPE. Truncated potentials may induce important
225 deviations to the calculated IFT values, as shown by several authors [53–57]. However,
226 these deviations are usually systematic, and the relative trends are maintained, specially
227 with similar systems. This study focuses on determining the qualitative effects of salt-
228 surfactant interactions (i.e., the IFT is increased or decreased), so the proper application
229 of the tail corrections would yield to the same qualitative conclusion. Nevertheless,

analytic tail corrections were included to the Lennard-Jones potential as recommended by TraPPE [58]. Finally, the long-range coulombic interactions were computed by means of the Particle-Particle/Particle-Mesh (PPPM) method [59].

IFT was calculated using the pressure tensor method of Kirkwood et al. [60, 61], which relates this property with the difference between the normal (P_{zz}) and tangential $\left(\frac{P_{xx}+P_{yy}}{2}\right)$ components of the pressure tensor (Eq. (3)). In this equation, L_z corresponds to the length of the simulation cell and the factor 1/2 arises since the simulation cell exhibits two interfaces. To calculate the statistical uncertainty of the results, three quasi-equivalent replicas of the same dodecane/water/surfactant system were built, using the same number of molecules, initial distribution, temperature and pressure. Then, all molecules are randomly rotated to generate a different initial state of the same system. The standard deviation of the three calculated IFT values are used as an estimate of the statistical uncertainty. Notice that all oil/water interfaces modelled in this work have a similar IFT, so the standard deviation of ± 0.8 dyn/cm calculated through this procedure is transferable to all simulations.

$$\gamma = \frac{L_z}{2}\left(P_{zz} - \frac{P_{xx}+P_{yy}}{2}\right) \tag{3}$$

The distribution of molecules along the z-direction of the simulation cell (i.e., the number density $\rho_i(z)$), was used to determine the accumulation or depletion of each species at the interface. To build them, the simulation cell was divided through the z-direction in bins of 1 Å width, and the different number of particles in each bin was averaged over the last 2 ns of the simulation. From the z-distributions the interfacial excess was calculated using Eq. (4) [32],

$$\Gamma_i^w = \int_a^b \frac{\rho_i(z) - \rho_i^{gibbs}(z)}{A} dz = \int_a^b \frac{\rho_i(z)}{A} dz - \frac{\bar{\rho}_i^w \cdot |\sigma^w - a| + \bar{\rho}_i^o \cdot |b - \sigma^w|}{A} \tag{4}$$

where the integration limits *a* and *b* are the center of the water and oil bulks respectively, and σ^w is the position of the Gibbs dividing surface. The position of σ^w was chosen to make the interfacial excess of water equal to zero, which was selected as the reference component. $\rho_i^{gibbs}(z)$ corresponds to the density profile of component *i* in a system with two bulk phases split with an infinitesimally thin interface. In this ideal system the density profile in each bulk phase is constant and equal to its the average density within the phase

($\bar{\rho}_i^w$ for water and $\bar{\rho}_i^o$ for oil). The water/dodecane reciprocal solubilities as well as the salt/dodecane solubilities are very low, so the term $\bar{\rho}_i^o$ can be neglected in our simulations. Finally, this integral is normalized by the interface unit area A.

To assess how the addition of salts and surfactants affects molecular interactions, Radial Distribution Functions (RDFs) between different molecular groups were calculated through VMD code [62]. Also, the orientation of surfactants at the interface was analyzed from the angle that both, the head and the tail groups, arrange with respect to the interfacial perpendicular axis (i.e., the z-axis).

3. Results and discussion

3.1. IFT calculations and identification of the salt-surfactant synergistic effect

We first performed MD simulations on pure water/dodecane systems with and without addition of salts at 300 K and 1 atm. These calculations were used as a benchmark to test the accuracy of the methodology and the different force fields in comparison to the experimental and simulation data available on simple systems. In the case of water/dodecane system, an equilibrium IFT value of 50.0 dyn/cm was obtained, in good agreement with reported experimental data (i.e., 51.2 – 52.3 dyn/cm [63, 64]).

Salts increase the equilibrium IFT because they stay at the bulk of the water phase yielding negative surface excess concentrations, which increase IFT according to Eq. (1). According to IFT results reported in the bibliography on water/oil systems with NaCl [65–68], $CaCl_2$ and $MgCl_2$ [69], IFT increases almost linearly at concentrations up to 2 molal. From the experimental linear trends, we should expect that in the case of NaCl $\Delta\gamma = \gamma_{salt} - \gamma_{no\_salt}$ values are between 3.0 ~~to~~ and 3.6 dyn/cm at 2 molal. On the other hand, both divalent salts should increase IFT a similar amount between 6.0 ~~to~~ and 6.5 dyn/cm at the same concentration.

Table 1 shows the equilibrium IFT results for the different water/salt/dodecane models by using different force fields along with their respective $\Delta\gamma$ values. $\Delta\gamma_{NaCl}$ is almost equivalent with the three force fields studied. CLAYFF and CHARMM increase IFT 3.7 dyn/cm and 3.1 dyn/cm, respectively, which is in good agreement with the expected values [65–69]. On the other hand, OPLS seems to slightly underestimate the NaCl effect showing a $\Delta\gamma_{NaCl} = 1.9$ dyn/cm. Although, the difference is small enough to consider these results comparable, other properties calculated in this work suggest that this underestimation might be important to reproduce some cross interactions (e.g., like surfactant-Na^+ interactions). These effects might be caused by a relatively low ε and high σ values of Na^+ OPLS parameters compared to the other force fields, which makes Na^+ to be more repulsive and to have less attractive crossed interactions. In the case of divalent salts, both CLAYFF and OPLS force fields are very similar, but they both give a higher $\Delta\gamma$ value for $CaCl_2$ than for $MgCl_2$ (i.e., $\Delta\gamma_{CaCl_2} = 7.1$ dyn/cm and $\Delta\gamma_{MgCl_2} = 5.6$ dyn/cm for CLAYFF; and $\Delta\gamma_{CaCl_2} = 7.2$ dyn/cm and $\Delta\gamma_{MgCl_2} = 4.6$ dyn/cm for OPLS). On the other hand, with CHARMM force field the IFT increase is equivalent for the three salts

297 studied (i.e., $\Delta\gamma_{NaCl} = 3.1$ dyn/cm, $\Delta\gamma_{CaCl_2} = 2.5$ dyn/cm and $\Delta\gamma_{MgCl_2} = 2.5$ dyn/cm).
298 From these results we can extract three premises: (i) NaCl is well reproduced with all
299 force fields but OPLS might be slightly underestimating the interactions between the Na^+
300 cation and other species; (ii) the divalent salts reproduced with CHARMM parameters
301 give IFTs too low when compared to experimental results [69]; and (iii) CLAYFF force
302 field seems give the best general representation of the three salts.

Table 1.
Equilibrium IFT results (in dyn/cm) for the water/salt/dodecane systems studied at 300 K and 1 atm using the three different force fields for salts. The values between parentheses correspond to the IFT change (*i.e.*, $\Delta\gamma = \gamma_{salt} - \gamma_{no\_salt}$). The estimated uncertainties in these simulations are $\pm$ 0.8 dyn/cm.

	Modelled system	No salt	NaCl	$CaCl_2$	$MgCl_2$
CLAYFF	Oil/water/salt	50.0	53.7 (3.7)	57.1 (7.1)	55.6 (5.6)
	+ $C_{12}E_3$	39.0	38.7 (-0.3)	45.4 (6.4)	43.4 (4.4)
	+ $(C_6C_5)CE_3$	39.0	35.5 (-3.5)	43.6 (4.6)	43.7 (4.7)
OPLS	Oil/water/salt	50.0	51.9 (1.9)	57.2 (7.2)	54.6 (4.6)
	+ $C_{12}E_3$	39.0	40.9 (1.9)	43.1 (4.1)	44.0 (5.0)
	+ $(C_6C_5)CE_3$	39.0	40.0 (1.0)	42.4 (3.4)	41.7 (2.7)
CHARMM	Oil/water/salt	50.0	53.1 (3.1)	52.5 (2.5)	52.5 (2.5)
	+ $C_{12}E_3$	39.0	39.1 (0.1)	43.0 (4.0)	41.7 (2.7)
	+ $(C_6C_5)CE_3$	39.0	36.9 (-2.1)	41.4 (2.4)	41.0 (2.0)

303

304 We would like to note that, even though force fields for salts do not usually use IFT as a
305 target function for fitting, the results obtained with the three force fields are reasonably
306 good. Also, the results obtained in our simulations do not state that CLAYFF is a better
307 force field than OPLS or CHARMM, but simply that in our system the least deviation
308 from the experimental results seems to be obtained by using CLAYFF parameters.
309 However, if other properties or systems were assessed, this could no longer be the case.
310 For the sake of simplicity, figures will show all the observed effects using only CLAYFF
311 parameters for salts, and the discussion among the different force fields will be reduced
312 to the minimum. All the information comparing the three force field calculations will be
313 available in the Supplementary Material.

314 After this preliminary evaluation, we assessed the effect of salt addition onto a
315 water/surfactant/dodecane system using low concentrations of a linear ($C_{12}E_3$) and a

ramified ($(C_6C_5)CE_3$) non-ionic surfactant. The pure water/dodecane IFT was reduced from the previous value of 50.0 dyn/cm to 39.0 dyn/cm when adding either the linear or the ramified surfactant. In these calculations all of the surfactant molecules stay at the interface with their polar heads facing the water phase and their tail groups oriented towards the dodecane phase.

The addition of salt upon these systems do not show the same trends that the pure water/dodecane system. When using CLAYFF force field and the linear $C_{12}E_3$ surfactant is present, the IFT is not increased by NaCl as before, denoting a cooperative effect between the surfactant and NaCl, which produces a small IFT reduction ($\Delta\gamma_{NaCl}$ = -0.3 dyn/cm). Additionally, if NaCl is into a system containing the ramified $(C_6C_5)CE_3$ surfactant, this cooperative effect is enhanced, and shows a larger reduction in the IFT value ($\Delta\gamma_{NaCl}$ = -3.5 dyn/cm). On the other hand, the interactions of these surfactants with divalent cations are weaker, and the calculated $\Delta\gamma$ does not achieve negative values. Even though divalent cations do not reduce the IFT, the $\Delta\gamma$ obtained is lower in presence of surfactants than in the pure dodecane/water system, which suggests that a weak interaction is still present on these systems. As an example, $CaCl_2$ in absence of surfactant gives a $\Delta\gamma_{CaCl_2}$ = 7.1 dyn/cm, whereas with the linear surfactant is $\Delta\gamma_{CaCl_2}$ = 6.4 dyn/cm and with the ramified surfactant is $\Delta\gamma_{CaCl_2}$ = 4.6 dyn/cm. The interaction is even weaker with $MgCl_2$, in which all $\Delta\gamma$ values are relatively similar. As a summary, the results obtained suggests that salts can interact with surfactants following the order of NaCl > $CaCl_2$ > $MgCl_2$ even when they do not explicitly show an absolute IFT reduction. Additionally, regardless of the salt used, the values of $\Delta\gamma$ tend to be ordered from the lowest to the highest as: $\Delta\gamma_{ramified} < \Delta\gamma_{linear} < \Delta\gamma_{no\_surfact}$, which suggest that the ramified surfactant is the molecule that interacts more strongly with salt ions, followed by the linear surfactant.

The same trends observed without surfactant, regarding IFT, are preserved in these simulations: the IFT reduction with NaCl is achieved also with CHARMM force field but not with OPLS, where the salt-surfactant interaction is the weakest. Similarly, divalent salts modelled with OPLS follow similar trends than CLAYFF, but the salt-surfactant interactions reproduced with CHARMM are almost inexistent.

The previous calculations suggest that the IFT in our system with surfactants is affected mainly by the presence of NaCl and secondarily by $CaCl_2$. The currently proposed

mechanisms (explained before) assume that IFT is reduced because, somehow, the concentration of surfactant is increased at the interface. However, in our setup all surfactant molecules are already accumulated at the interface before adding the salt, so the effect must be explained from other molecular rearrangements, orientations, or microscopical interactions. In this sense, in the following sections we will analyze different factors that could be affecting the IFT and comparing the effects depending on the salt used.

3.2. Interfacial excess concentrations and z-distributions:

According to Eq. (1), the γ of a system depends on the interfacial excess of each added species. This magnitude can be positive if the compound accumulates at the interface, whereas it can be negative if it avoids the interface and stays at the bulk of its phase. We calculated the interfacial excess of both salt and surfactants from the z-distributions at equilibrium by means of Eq. (4), using as integration limits the center of each liquid phase. As all surfactant molecules stay at the interface for the whole simulation time, their density at the bulk is equal to 0, and the interfacial excess is the same for all calculations (i.e., $\rho_i^{gibbs}(z) = 0$ and $\Gamma_i^w = 1.50$ μmol/m^2).

For the water/salt/dodecane systems (i.e., without surfactants), the interfacial excess of salts is always negative, which justifies the increase of the IFT. According to our results, the IFT change with the interfacial excess cannot be directly compared between different species. For example, with CLAYFF force field (Table 2), both Ca^{2+} and Cl^- have a interfacial excess of $\Gamma_+^w = -0.45$ μmol/m^2 and $\Gamma_-^w = -0.89$ μmol/m^2 respectively, whereas Mg^{2+} and Cl^- have $\Gamma_+^w = -0.92$ μmol/m^2 and $\Gamma_-^w = -1.83$ μmol/m^2 respectively. If we only considered the interfacial excess of $CaCl_2$ and $MgCl_2$ we would conclude that $MgCl_2$ is farther from the interface than $CaCl_2$, so the change in IFT when adding $MgCl_2$ should be larger. However, with all the checked force fields $\Delta\gamma_{CaCl_2} > \Delta\gamma_{MgCl_2}$, or at least equal, as it can be seen in Table 1.

The interfacial excess of salts is generally increased by the presence of surfactants following the order $\Gamma_{salt}^w(no\_surfact.) < \Gamma_{salt}^w(C_{12}E_3) < \Gamma_{salt}^w((C_6C_5)CE_3)$. This implies that the polar head groups of surfactants are interacting with the ions of salts, attracting them to the interface. Also, the ramified surfactant is more effective than the

linear surfactant as it can be seen with all studied force fields in Table 2. These trends correlate with the respective values of Δγ obtained in section 3.1, suggesting again that $(C_6C5)CE_3 > C_{12}E_3$ and $NaCl > CaCl_2 > MgCl_2$ for the salt-surfactant synergistic effects in the studied system. Notice from Table 2 that the addition of NaCl onto systems with these non-ionic surfactants can even yield positive interfacial excesses. The calculations with positive Γ_i^w are the same ones that gave negative or almost zero values of Δγ. Finally, similar trends regarding the other force fields are shown again, producing weaker effects for the NaCl/OPLS and $CaCl_2$/$MgCl_2$/CHARMM force field combinations.

Table 2.
Gibbs interfacial excess concentrations in μmol/m^2 for the cation (Γ_+^w) and the anion (Γ_-^w) of all studied systems at 300 K and 1 atm.

	Modelled system	NaCl		$CaCl_2$		$MgCl_2$	
		Γ_+^w	Γ_-^w	Γ_+^w	Γ_-^w	Γ_+^w	Γ_-^w
CLAYFF	Oil/water/salt	-0.83	-0.82	-0.45	-0.89	-0.92	-1.83
	+ $C_{12}E_3$	0.20	0.23	-0.29	-0.57	-0.89	-1.75
	+ $(C_6C_5)CE_3$	0.22	0.29	-0.19	-0.46	-0.76	-1.51
OPLS	Oil/water/salt	-0.38	-0.40	-0.85	-1.64	-0.99	-1.99
	+ $C_{12}E_3$	-0.51	-0.54	-0.17	-0.34	-0.61	-1.12
	+ $(C_6C_5)CE_3$	-0.31	-0.30	-0.14	-0.29	-0.45	-0.95
CHARMM	Oil/water/salt	-0.54	-0.51	-0.54	-1.12	-1.07	-2.11
	+ $C_{12}E_3$	0.25	0.31	-0.58	-1.19	-1.19	-2.40
	+ $(C_6C_5)CE_3$	0.47	0.44	-0.66	-1.35	-0.93	-1.87

In Fig. 2 one can see the z-distributions of all studied systems. In absence of surfactant (Fig. 2a-c) the concentration of the three salts in dodecane is zero and then, it starts increasing in the water phase until the bulk concentration. In these systems each Na^+ cation is paired with a single Cl^- anion in the whole simulation cell, whereas Ca^{2+} and Mg^{2+} are paired with two Cl^- due to its divalent charge. However, if we add a non-ionic surfactant onto a cell with NaCl (Fig. 2d and Fig. 2g), the salt z-distribution at the oil/water interface changes significantly. Two very well-defined peaks (per interface) appear in the distribution: the first is a Na^+ peak very close to the interface that suggest that the polar head groups of the surfactant are attracting the cation, increasing the interfacial excess and reducing the IFT. The second is the most intern Cl^- peak,

approximately 5 Å away from the Na^+ peak, facing the water bulk. This group of ions do not interact with the surfactants as strongly as Na^+, so they have been dragged towards the interface by the coulombic force of its counterions. These differences in interaction strengths induce a different ionic distribution for Na^+ and for Cl^- at the interface, effectively producing an electric double layer, which makes the interface more polar and probably also affects the IFT (i.e., see the magnifications of Fig. 2d and Fig. 2g). The excess concentrations of divalent cations are also increased by the presence of surfactant (Table 2), but their interaction is much weaker, and their distributions do not change significantly (i.e., no differences can be appreciated in Fig. 2b-c Fig. 2e-f and Fig. 2h-g due to weaker salt-surfactant interactions).

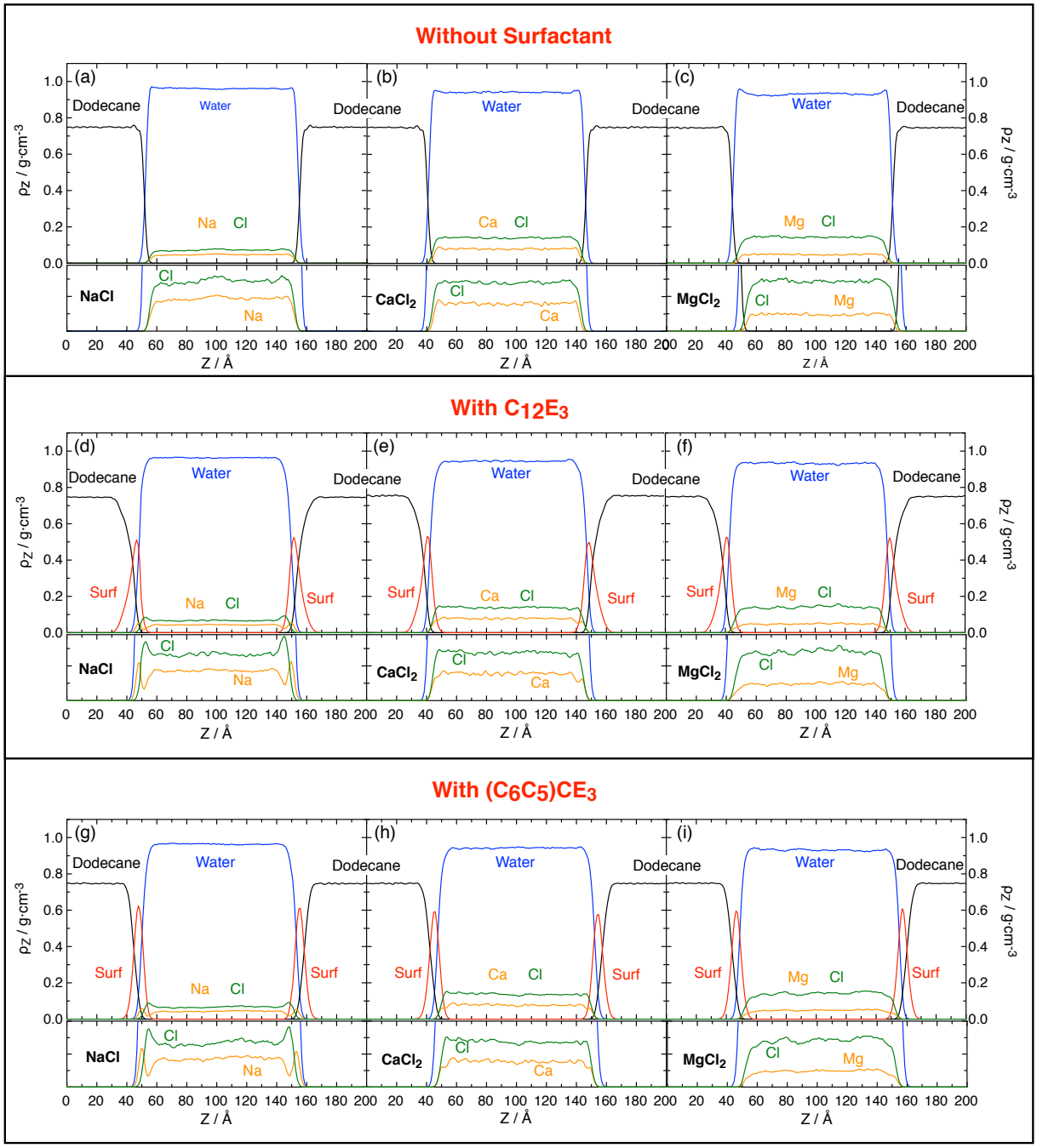

Fig. 2. The z-distributions of water/salt/dodecane systems, with and without surfactant, at equilibrium. The top row (*i.e.*, (a), (b) and (c)) represents the system only with salt (*i.e.*, NaCl, $CaCl_2$ and $MgCl_2$, respectively and without surfactant); the mid row (*i.e.*, (d), (e) and (f)) shows the distributions of the systems with the linear $C_{12}E_3$ surfactant and the three salts; and the bottom row (*i.e.*, (g), (h) and (i)) contains the equilibrium configurations of systems with the ramified $(C_6C_5)CE_3$ surfactant and the salts. Below each subplot there is a zoom to see more clearly the salt distribution, in which surfactant and dodecane distributions were erased for clarity. In all plots blue lines correspond to water, black lines to dodecane, red lines to the surfactant and orange/green lines to the cation/anion of each salt, respectively. The results shown are calculated with CLAYFF force field for salts at 300 K and 1 atm.

408

409 The obtained results in this section show that cations can interact with the surfactant head
410 groups, which affect the distributions of salt ions at the interface. These interactions are

stronger in salts that showed the strongest IFT reductions (e.g., the case of Na^+ in Fig. 2d and Fig. 2g). In these situations, the interface even becomes polarized by an electric double layer of Na^+ and Cl^- ions. To conclude, there is a correlation between the reorganization of interfacial cations and the IFT reduction effect. However, this is not enough to explain the salt-surfactant synergistic effect. Specifically, the IFT reduction also depends on the surfactant used, as suggested by the results compiled in Table 1 and Table 2.

This IFT reduction is relatively weak when compared to the required synergistic effects needed for efficient EOR. However, the effect seen in this work is comparable to some of the abovementioned studies that use different surfactants and brines and can shed some light in explaining previously published experiments. Some examples are: Al-Sahhaf et al. [11] found IFT reductions of 2-3 dyn/cm when adding salt to both a cationic and an anionic surfactant, or Fainermann et al. [14], who showed that NaCl was capable of reducing the IFT of an oil/water /surfactant system between 5 dyn/cm and 18 dyn/cm depending on the surfactant concentration. The synergistic effect with non-ionic surfactants + NaCl has also been experimentally described close to the CMC by Bera et al. [12], even achieving resulting IFTs lower than 0.1 dyn/cm.

3.3 Surfactant orientation at the interface

Normally, the IFT of a system is reduced when compounds accumulate at the interface, but some works have proven that the orientation of some species can also be an important aspect to consider. In fact, the orientation of liquid crystals dramatically changes the interfacial tension (i.e., the reader is redirected to Refs. [70, 71] for a recent review of this topic). To evaluate the effect that salt ions produce towards surfactant orientation the angle between the head and the tail groups with respect to the perpendicular of the interfacial plane (i.e., the z-axis in our simulation cell) was analyzed. Both non-ionic surfactants have relatively long heads and tails, so the orientation of each group was determined separately, as it can be seen in Fig. 3. The director vector of the head group was calculated, from principal component analysis, considering the molecular axis that goes in the direction from the first oxygen atom (i.e., the closest to the tail group) to the terminal OH group. Similarly, the tail group vector was chosen as the molecular axis that follows the direction from the first atom of the tail (i.e., the CH_x bonded to the first

oxygen) to the terminal CH_3 group. For the case of the ramified surfactant, each tail was considered separately. Moreover, to get information about the conformation of the surfactants at the interface, we computed the angle formed between the different groups within the same molecule (i.e., the head-tail angle for both surfactants, and the tail-tail angle for the ramified surfactant).

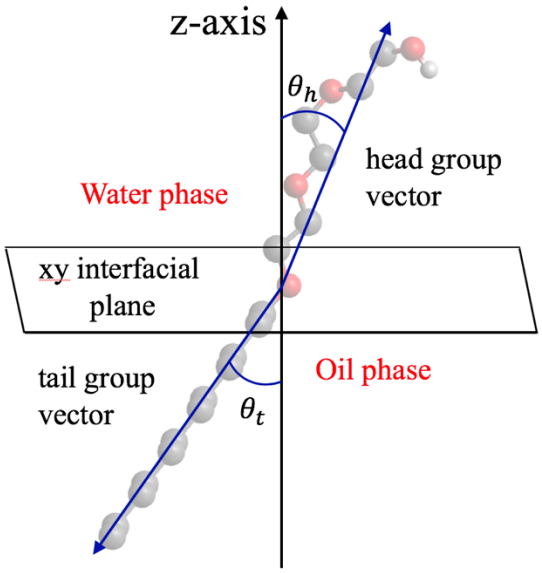

Fig. 3. Intramolecular reference framework used for angular distributions of the tail and the head groups of surfactant molecules at the interface.

Fig. 4 shows the angular distribution of head and tail groups for both the linear surfactant (Fig. 4a-c) and the ramified surfactant (Fig. 4d-f) in absence and presence of salt. It is worth noting that in all simulations the head groups are facing the water phase, whereas the tail groups are facing the oil phase. In absence of salt, the head groups of both surfactants (Fig. 4a and Fig. 4d) have the highest probability to be oriented almost parallel to the interfacial plane (i.e., between 70º and 90º with respect to the perpendicular axis). On the other hand, the tail groups for the linear $C_{12}E_3$ (Fig. 4b) show a uniform random distribution at angles between 40º and 90º with respect to the z-axis, whereas the tail groups of the ramified $(C_6C_5)CE_3$ (Fig. 4e) have a large probability to be oriented between 60º and 90º. The obtained results show that both surfactants are positioned relatively planar with respect to the interface, specially the surfactant head groups and the tail groups of the ramified surfactant. This means that the ramified surfactant should occupy more interfacial area than the linear surfactant, because it spreads more through the interface rather than pointing towards the dodecane bulk. This effect was also observed

in the z-distributions of Fig. 2, where the ramified surfactant distribution peak is thinner than the one for the linear surfactant. Finally, the angle between the head and the tail groups for both $C_{13}E_3$ (Fig. 4c) forms a very wide distribution with the maximum of probability located at values from 80º to 130º approximately, which suggests that the surfactant is significantly bent (i.e., 180º would be completely linear). On the other hand, $(C_6C_5)CE_3$ presents an even flatter distribution with similar probabilities between 30º and 140º. Notice that all distributions shown here are relatively flat because surfactant concentration is very low. This fact implies that surfactant molecules are relatively free at the interface and their orientation is not restricted by the presence of other surface-active molecules.

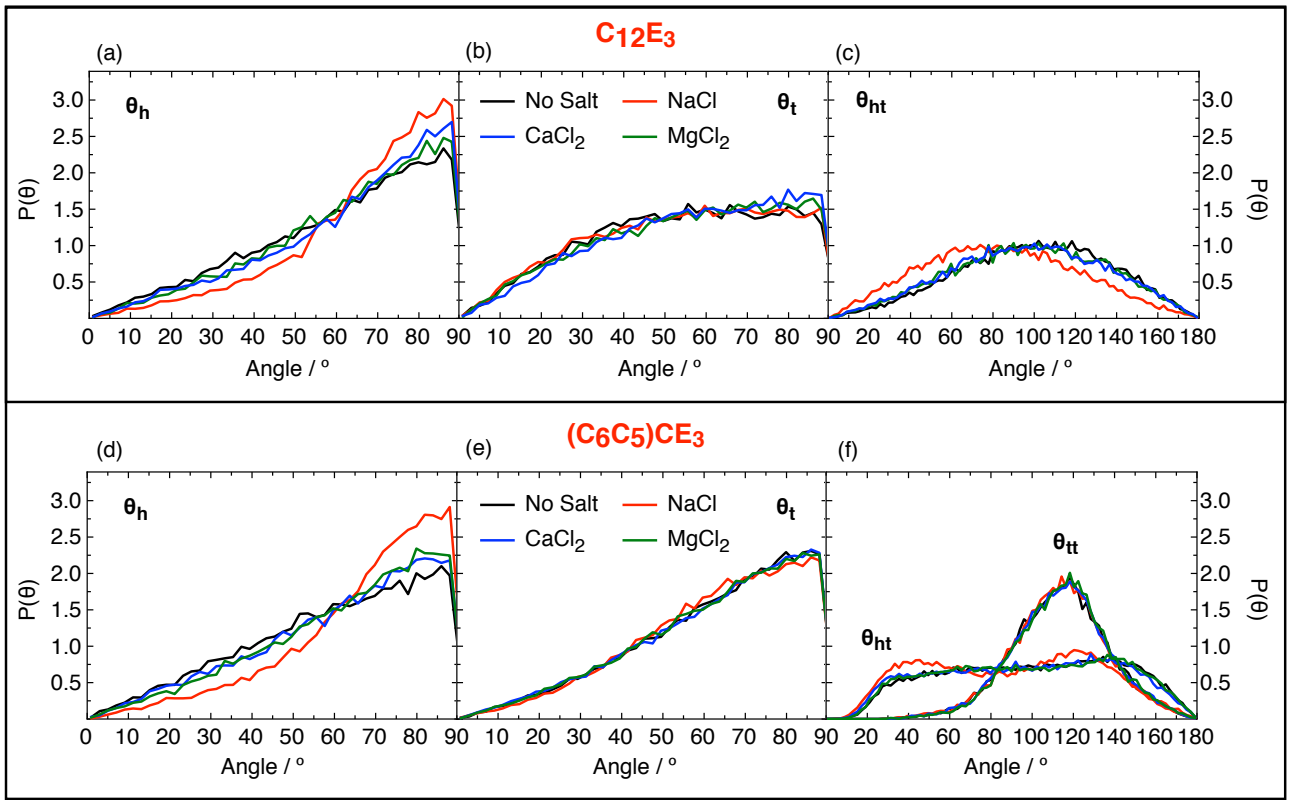

Fig. 4. Probability angular distributions for different groups in the linear surfactant ($C_{12}E_3$) and in the ramified surfactant ($(C_6C_5)CE_3$). The distribution of head groups (θ_h) is shown in (a) and (d), the distribution of tail groups (θ_t) is depicted in (b) and (e) and the head/tail (θ_{ht}) and tail/tail (θ_{tt}) angles are compiled in (c) and (f). The results correspond to the simulations performed with CLAYFF force field for salts at 300 K and 1 atm.

The addition of salt onto the system with surfactants does not affect the distribution of any tail groups (i.e., no effects are seen in Fig. 4b and Fig 4e). However, the peak between 70º and 90º of the head group distribution is increased in the order NaCl > $CaCl_2$ > $MgCl_2$, as shown in Fig. 4a and Fig. 4d. Namely, this probability is increased around a 30% with

both surfactants when adding NaCl. This implies again that cations are able to interact with the surfactant head groups and, in average, make them become more planar towards the interface. In general, there is a clear correlation between the amplitude of this effect and the IFT reduction, which is more noticeable when adding NaCl. Additionally, as the head group angle is changing, the angle between the head and the tail groups also changes. In particular, the surfactants become more bent by effect of salts.

According to the results shown in this section, the orientations of surfactant head and tail groups at low interfacial concentration are relatively planar. In fact, the highest probability in their angular distribution with respect the z-axis for both groups is over 45º. Also, the ramified surfactant tail occupies more interfacial area than its linear counterpart, which implies that it should be more effective in covering the water/oil interface and in reducing the IFT. On the other hand, the distribution of head groups in both surfactants is affected similarly by salinity. The head groups became more planar with respect to the interface after the addition of NaCl, but as the ramified surfactant tail occupies more interfacial area it reduces the IFT more effectively. Finally, tail groups were not affected by the presence of salt.

3.4 Radial distribution functions

We have seen in the previous sections that both, surfactants and salts are forcing each other to rearrange at the interface. In fact, we have observed a correlation between the amplitude of the IFT reduction effect in surfactant/NaCl mixtures (Table 1), the formation of the electric double layer by interfacial Na^+ and Cl^- ions (Table 2 and Fig. 2) and the bending of surfactant head groups (Fig. 4). To know more about the interactions that drive these general patterns we have calculated the RDFs between different molecular groups (i.e., the water, the salt ions, the dodecane and the surfactant head and tail groups) and compared their interactions in absence and presence of salt.

First, we compared how the RDF between water and dodecane molecules close to the interface was affected by salinity for systems with and without surfactants. We have considered all atoms in dodecane and only O atoms for water when building the pair-wise distributions. The system without surfactant (Fig. 5a) shows an exactly equivalent distribution regardless of the salt used, which means that salinity does not affect

water/dodecane interactions. However, the systems with both the linear (Fig. 5b) and the ramified (Fig. 5c) surfactants with NaCl, show a slightly lower RDF. This fact implies that dodecane and water are, in average, farther away from each other because surfactants occupy more interfacial area. This relegates dodecane and water molecules to their respective bulks reducing the RDF. Specifically, the dodecane/water RDFs when including surfactants and NaCl are reduced approximately a 15% and a 30% for the linear and ramified surfactants, respectively. Notice that Ca^{2+} is also able to separate the dodecane and water phases with the linear surfactant (Fig. 5b), as well as it was also able to affect the orientation of the linear surfactant at the interface (Fig. 4a).

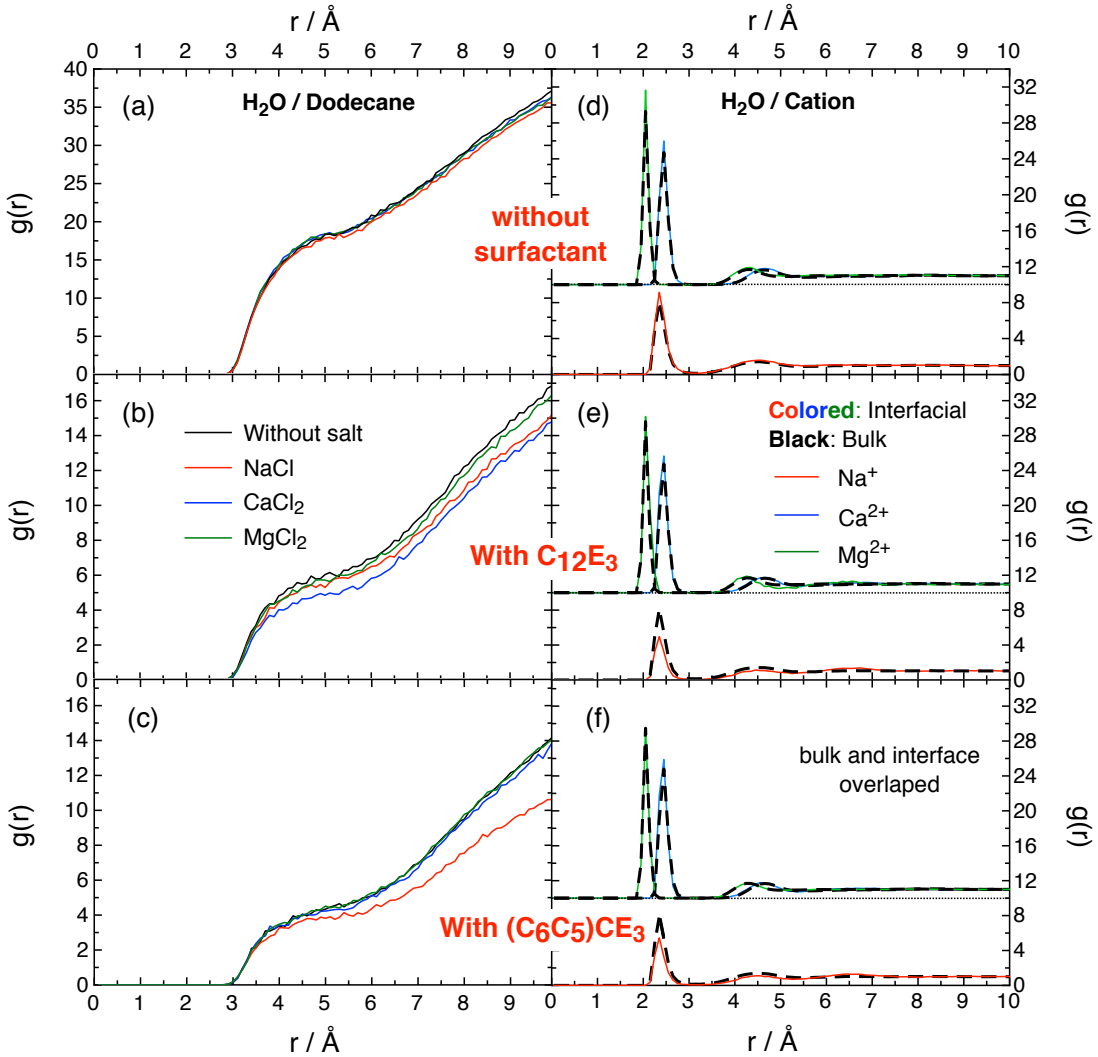

Fig. 5. In (a), (b) and (c) water/dodecane RDFs and in (d), (e) and (f) water/cation RDFs for molecules close to the interface in systems with and without surfactants. The black dashed lines in (d), (e) and (f) refer to the RDF of species at bulk. To build the pair-wise distributions for molecular groups, we considered the O atoms for water and the 12 CH_x groups for dodecane. The results correspond to the simulations performed with CLAYFF force field for salts at 300 K and 1 atm.

519 Then, we analyzed how the coordination spheres of interfacial cations were perturbed
520 with respect the cations at the bulk. To that end, water/cation RDFs were built
521 differentiating two regions: (i) the water bulk and (ii) the interface. The interface cations
522 were selected by listing all Na^+, Ca^{2+} or Mg^{2+} located at less than 15 Å from any dodecane
523 molecule, which means that are at 15 Å from the oil phase. The rest are considered bulk
524 cations. In absence of surfactant (Fig. 5d), there is no difference between the coordination
525 spheres of interfacial or bulk cations. However, in presence of any surfactant (Fig. 5e and
526 Fig. 5f), the solvation spheres of interfacial Na^+ are reduced a 40 % with respect bulk
527 Na^+. This result suggests that Na^+ is losing part of its solvation sphere to interact closely
528 with the surfactant. Notice that this is a necessary process to induce salt-surfactant
529 synergistic effects because water layers screen the electrostatic charges of ions in
530 solution, weakening the interactions between salt ions and surfactants. On the other hand,
531 this effect is not seen with Ca^{2+} and Mg^{2+} because their interactions with water are too
532 strong to be broken. Concretely, Na^+ has a relatively weak hydration sphere with a
533 hydration enthalpy of -98 kcal/mol [72], whereas Ca^{2+} or Mg^{2+} have -377 and -459
534 kcal/mol, respectively [72]. These experimental information of hydration enthalpies
535 support the conclusion that the surfactant is capable of breaking part of the hydration
536 sphere of Na^+ but is not strong enough to separate the divalent cations from their hydration
537 sphere, as seen by water/cation RDFs.

538 Fig. 6 shows the more relevant changes due to salinity in RDFs of a system with each
539 surfactant. First, (Fig. 6a and Fig. 6b) show the distributions between water and the
540 surfactant head groups, where large peaks appear at 2.75 Å, denoting the average
541 interacting distance between water and the head groups. $MgCl_2$ does not affect water-
542 surfactant interactions (i.e., the distribution is identical to the RDF without salt), which
543 implies that it interacts very weakly with the head groups, followed by $CaCl_2$ (i.e., the
544 peak in the distribution is slightly lower than with $MgCl_2$). However, this peak disappears
545 completely in presence of NaCl, which suggest that Na^+ is sequestering the surfactant
546 head groups to prevent water/surfactant interactions. Notice that the systems with IFT
547 reduction effects are also the ones where the cation and the surfactant lose their solvation
548 sphere to interact with each other.

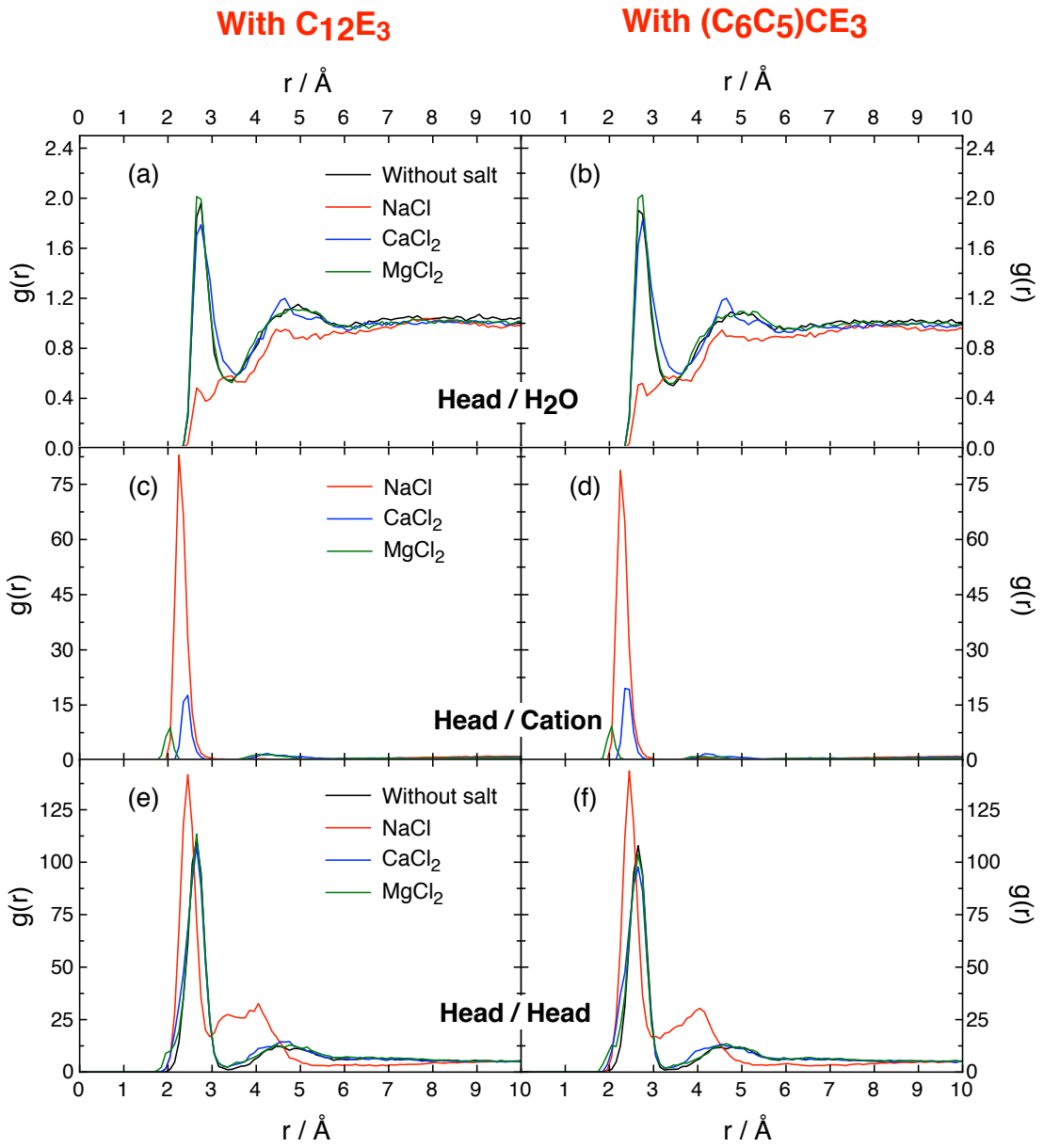

Fig. 6. RDF between surfactant head groups and water (a,b), head groups and the cations (c,d) or head groups with other head groups (e,f). To build the pair-wise distribution for molecular groups, we considered the O atoms for water and the O of the head groups for the surfactant heads. The results correspond to the simulations performed with CLAYFF force field for salts at 300 K and 1 atm.

549

550 Then, if we evaluate the distributions between the head groups and the ions (Fig. 6c and
551 Fig. 6d) we confirm the previous affirmation. Na^+ forms a very high and narrow peak at
552 2.25 Å, which denotes the strong salt-surfactant interaction. $CaCl_2$ and $MgCl_2$ form peaks
553 in similar position but significantly lower in height, following the same trend than in Fig.
554 6a-b (i.e., Ca^{2+} has a stronger interaction with the surfactant head groups than Mg^{2+}).
555 From these results, we can conclude that the surfactant head group is the responsible
556 moiety that interacts with Na^+ and force it to release from its hydration sphere.

Finally, salinity also affects how surfactants are arranged among themselves. In Fig. 6e and Fig. 6f one can see the head-head group distributions that, in absence of salt, form a high peak at 2.65 Å and a wider lower peak around 4.75 Å. However, in the presence of NaCl the first peak is displaced to 2.45 Å and the 2^{nd} peak to less than 4 Å, increasing both peaks in height. This result suggests that NaCl not only sequestrates the head groups from water, but also brings surfactants closer to each other (i.e., an enhanced interfacial packing).

Notice that the enhanced packing here validated, was already proposed by experimentalists to explain IFT reduction through a larger accumulation of surfactants at the interface [20, 21]. However, in our MD simulations all surfactant molecules are already at the interface and the IFT is still reduced, which suggests that the salt-surfactant synergistic effect also includes all phenomena described throughout this work. Additionally, the change of environment around the surfactant head groups (i.e., less surfactant/water interactions) does not imply that the surfactant is losing its interfacial activity, but it just interacts strongly with the cations that form the electric double layer at the interface.

The results obtained in this final section suggest that Na^+ is releasing from its hydration shell to strongly interact with the surfactant head groups, effectively sequestrating them from water. The new arrangement between surfactants and salt forces the head groups to be more planar with respect to the interfacial plane, occupying more area and slightly expelling dodecane molecules from the interface, which increases the efficiency of the surfactant. Similar effects are seen with Ca^{2+} but in a much weaker extent, whereas Mg^{2+} is almost not modifying any salt-surfactant interfacial property, ranking the effects as $Na^+ > Ca^{2+} > Mg^{2+}$. The aforementioned interactions also induce a tighter packing of the surfactant head groups. This packing could potentially allow additional surfactant molecules to accumulate at the interface to further reduce the IFT, which is a mechanism that was already deduced from experimental observations, and is here validated through molecular dynamics simulations.

4. Conclusion

With the aim of explaining the experimentally observed salt-surfactant synergistic effect from a microscopic point of view we have performed MD simulations to study how different salts (i.e., NaCl, $CaCl_2$ and $MgCl_2$) affect the interfacial properties of three different systems: (i) a pure water/dodecane system, (ii) the same system with additional linear non-ionic surfactants (i.e., water/dodecane/$C_{12}E_3$) and (iii) the first system with additional ramified non-ionic surfactants (i.e., water/dodecane/$(C_6C_5)CE_3$). In this study we have been able to confirm that salt ions are capable of interacting with the surfactants changing their interfacial molecular distribution and thus affecting the IFT.

In summary, we have observed that cations can potentially release from its hydration sphere to interact with the surfactant head groups preventing surfactant-water interactions. These interactions affect the surfactant distributions at the interface, reducing the distance between surfactant head groups. This mechanism was proposed experimentally and is validated by the currently MD simulations but is not sufficient to explain the salt-surfactant synergistic effect on its own. Other processes are involved in lowering the IFT below the CMC, such as the more planar distribution of surfactants in presence of salt. Altogether, below the CMC, salinity helps the surfactants to rearrange and occupy more interfacial area, reducing the water/dodecane interactions and ultimately decreasing the IFT. The strong attraction felt by cations towards the surfactant molecules can lead to an increase of the interfacial excess of the salt, even achieving positive values for the Γ_{salt}^{w} (i.e., instead of the common negative values). From these results one can conclude that salt ions could (in certain conditions) accumulate at the interface and contribute to the IFT reduction as any other surface-active compound. On the other hand, anions feel less attraction from the surfactants than cations, which generates an electric double layer that polarizes the interface, being a possible additional cause of IFT reduction. The effects observed are not equivalent with all cations. Specifically, Na^+ seems to be the strongest interaction moiety because it can release from its hydration sphere more easily, whereas Ca^{2+} and Mg^{2+} present significantly weaker salt-surfactant interactions because their coulombic interactions become screened by their strongly bonded solvation water molecules. This ranks the salt-surfactant synergistic effect in this particular system to be $Na^+ > Ca^{2+} > Mg^{2+}$. Finally, the ramified surfactant is more effective than the linear surfactant in occupying the interface, which makes the salt-surfactant synergistic effect more noticeable.

All of the previously described effects are capable of slightly reducing the IFT of the system by a relatively small amount and are not capable of achieving ultralow IFT on their own. For this reason, even though the salt-surfactant effect here described works in favor of oil recovery, it could be easily overcome by other interactions that hamper oil extraction in high salinity environments.

Declaration of Competing Interest

The authors have no competing of interests to declare.

Acknowledgments

This work was supported by the Spanish *Ministerio de Economía y Competitividad* grant (RTI2018-094757-B-I00), the Spanish *Structures of Excellence María de Maeztu* program through grant MDM-2017-0767 and the *Generalitat de Catalunya* grants (2014SGR1582, 2017SGR13, and XRQTC). G.A. thanks the University of Barcelona for both the APIF predoctoral grant and the APIF stay grant at Universidad de Concepción (Chile).

Appendix A. Supplementary material

Supplementary material to this article can be found online at: _____

References

[1] J.J. Sheng, Status of surfactant EOR technology, Petroleum. 1 (2015) 97–105.

[2] M.S. Kamal, I.A. Hussein, A.S. Sultan, Review on Surfactant Flooding: Phase Behavior, Retention, IFT, and Field Applications, Energ. Fuel. 31 (2017) 7701–7720.

[3] B. Song, X. Hu, X. Shui, Z. Cui, Z. Wang, A new type of renewable surfactants for enhanced oil recovery: Dialkylpolyoxyethylene ether methyl carboxyl betaines, Colloid. Surface. A. 489 (2016) 433–440.

[4] N. Morrow, J. Buckley, Improved Oil Recovery by Low-Salinity Waterflooding, J. Pet. Technol. 63 (2011) 106–112.

[5] P.P. Jadhunandan, Effects of Brine Composition, Crude Oil, and Aging Conditions on Wettability and Oil Recovery, PhD Dissertation, New Mexico Institute of Mining & Technology, 1990.

[6] W. von Rybinski, B. Guckenbiehl, H. Tesmann, Influence of Co-Surfactants on Microemulsions with Alkyl Polyglycosides, Colloid. Surface. A. 142 (1998) 333–342.

[7] Lu, J., Development of Novel Surfactants and Methods for Chemical Enhanced Oil Recovery, PhD Dissertation, University of Texas, 2014.

[8] Z. Jeirani, B. Mohamed Jan, B. Si Ali, I.M. Noor, C.H. See, W. Saphanuchart, Formulation, Optimization and Application of Triglyceride Microemulsion in Enhanced Oil Recovery, Ind. Crops Prod. 43 (2013) 6–14.

[9] A.E. Silva, G. Barratt, M. Chéron, E.S.T. Egito, Development of Oil-in-Water Microemulsions for the Oral Delivery of Amphotericin B, Int. J. Pharm. 454 (2013) 641–648.

[10] A.M. Howe, A. Clarke, J. Mitchell, J. Staniland, L. Hawkes, C. Whalan, Visualising Surfactant Enhanced Oil Recovery, Colloid. Surface. A. 480 (2015) 449–461.

[11] T. Al-Sahhaf, A. Elkamel, A.S. Ahmed, A.R. Khan, The Influence of Temperature, Pressure, Salinity, and Surfactant Concentration on the Interfacial Tension of the N-Octane-Water System, Chem. Eng. Commun. 192 (2005) 667–684.

[12] A. Bera, A. Mandal, B.B. Guha, Synergistic Effect of Surfactant and Salt Mixture on Interfacial Tension Reduction between Crude Oil and Water in Enhanced Oil Recovery, J. Chem. Eng. Data. 59 (2014) 89–96.

[13] X. Chen, S.S. Adkins, Q.P. Nguyen, A.W. Sanders, K.P. Johnston, Interfacial Tension and the Behavior of Microemulsions and Macroemulsions of Water and Carbon Dioxide with a Branched Hydrocarbon Nonionic Surfactant, J. Supercrit. Fluids. 55 (2010) 712–723.

[14] V.B. Fainerman, S.V. Lylyk, E.V. Aksenenko, N.M. Kovalchuk, V.I. Kovalchuk, J.T. Petkov, R. Miller, Effect of Water Hardness on Surface Tension and Dilational Visco-Elasticity of Sodium Dodecyl Sulphate Solutions, J. Colloid Interface Sci. 377 (2012) 1–6.

[15] A. Ge, Q. Peng, H. Wu, H. Liu, Y. Tong, T. Nishida, N. Yoshida, K. Suzuki, T. Sakai, M. Osawa, S. Ye, Effect of Functional Group on the Monolayer Structures of Biodegradable Quaternary Ammonium Surfactants, Langmuir. 29 (2013) 14411–14420.

[16] T. Jiao, X. Liu, J. Niu, Effects of Sodium Chloride on Adsorption at Different Interfaces and Aggregation Behaviors of Disulfonate Gemini Surfactants, RSC Adv. 6 (2016) 13881–13889.

[17] A.M. Johannessen, K. Spildo, Enhanced Oil Recovery (EOR) by Combining Surfactant with Low Salinity Injection, Energ. Fuel. 27 (2013) 5738–5749.

685 [18] P. Koelsch, H. Motschmann, Varying the Counterions at a Charged Interface,
686 Langmuir. 21 (2005) 3436–3442.

687 [19] S. Kumar, A. Mandal, Studies on Interfacial Behavior and Wettability Change
688 Phenomena by Ionic and Nonionic Surfactants in Presence of Alkalis and Salt for
689 Enhanced Oil Recovery, Appl. Surf. Sci. 372 (2016) 42–51.

690 [20] Z. Liu, Z. Li, X. Song, J. Zhang, L. Zhang, L. Zhang, S. Zhao, Dynamic Interfacial
691 Tensions of Binary Nonionic–Anionic and Nonionic Surfactant Mixtures at Water–
692 Alkane Interfaces, Fuel. 135 (2014) 91–98.

693 [21] Z. Liu, L. Zhang, X. Cao, X. Song, Z. Jin, L. Zhang, S. Zhao, Effect of Electrolytes
694 on Interfacial Tensions of Alkyl Ether Carboxylate Solutions, Energ. Fuel. 27 (2013)
695 3122–3129.

696 [22] K. Staszak, D. Wieczorek, K. Michocka, Effect of Sodium Chloride on the
697 Surface and Wetting Properties of Aqueous Solutions of Cocamidopropyl Betaine, J.
698 Surfactants Deterg. 18 (2015) 321–328.

699 [23] A. Witthayapanyanon, E.J. Acosta, J.H. Harwell, D.A. Sabatini, Formulation of
700 Ultralow Interfacial Tension Systems Using Extended Surfactants, J. Surfactants Deterg.
701 9 (2006) 331–339.

702 [24] H. Francke, M. Thorade, Density and Viscosity of Brine: An Overview from a
703 Process Engineers Perspective, Chem. Erde - Geochem. 70 (2010) 23–32.

704 [25] O. Ozdemir, S.I. Karakashev, A.V. Nguyen, J.D. Miller, Adsorption and Surface
705 Tension Analysis of Concentrated Alkali Halide Brine Solutions, Miner. Eng. 22 (2009)
706 263–271.

707 [26] A.A. Zavitsas, Properties of Water Solutions of Electrolytes and Nonelectrolytes,
708 J. Phys. Chem. B. 105 (2001) 7805–7817.

709 [27] H. Aghdastinat, S. Javadian, A. Tehrani-Bagha, H. Gharibi, Spontaneous
710 Formation of Nanocubic Particles and Spherical Vesicles in Catanionic Mixtures of Ester-
711 Containing Gemini Surfactants and Sodium Dodecyl Sulfate in the Presence of
712 Electrolyte, J. Phys. Chem. B. 118 (2014) 3063–3073.

713 [28] P. Mukerjee, C.C. Chan, Effects of High Salt Concentrations on the Micellization
714 of Octyl Glucoside: Salting-Out of Monomers and Electrolyte Effects on the
715 Micelle−Water Interfacial Tension, Langmuir. 18 (2002) 5375–5381.

716 [29] V. Seredyuk, E. Alami, M. Nydén, K. Holmberg, A.V. Peresypkin, F.M. Menger,

717 Adsorption of Zwitterionic Gemini Surfactants at the Air–Water and Solid–Water
718 Interfaces, Colloid. Surface. A. 203 (2002) 245–258.
719 [30] Z. Zhao, C. Bi, Z. Li, W. Qiao, L. Cheng, Interfacial Tension Between Crude Oil
720 and Decylmethylnaphthalene Sulfonate Surfactant Alkali-Free Flooding Systems,
721 Colloid. Surface. A. 276 (2006) 186–191.
722 [31] H. Schott, Saturation Adsorption at Interfaces of Surfactant Solutions, J. Pharm.
723 Sci. 69 (1980) 852–854.
724 [32] J. W. Gibbs, The Colected Works of J. W. Gibbs, Longmans Green, New York,
725 1931.
726 [33] C. Yang, W. Lin, Q. Wang, B. Niu, X. He, Inorganic Salts Effect on Adsorption
727 Behavior of Surfactant AEC at Liquid/Liquid Interface, Res. J. Appl. Sci. Eng. Technol.
728 6 (2013) 1424–1427.
729 [34] T. Zhao, G. Xu, S. Yuan, Y. Chen, H. Yan, Molecular Dynamics Study of Alkyl
730 Benzene Sulfonate at Air/Water Interface: Effect of Inorganic Salts, J. Phys. Chem. B.
731 114 (2010) 5025–5033.
732 [35] S. Yuan, Y. Chen, G. Xu, Molecular Dynamics Studies on Octadecylammonium
733 Chloride at the Air/Liquid Interface, Colloid. Surface. A. 280 (2006) 108–115.
734 [36] Q. Xie, Y. Chen, L. You, M.M. Hossain, A. Saeedi, Drivers of Wettability
735 Alteration for Oil/Brine/Kaolinite System: Implications for Hydraulic Fracturing Fluids
736 Uptake in Shale Rocks, Energies. 11 (2018) 1666:1–13.
737 [37] S. Plimpton, Fast Parallel Algorithms for Short-Range Molecular Dynamics, J.
738 Comput. Phys. 117 (1995) 1–19.
739 [38] W. Wagner, A. Pruß, The IAPWS Formulation 1995 for the Thermodynamic
740 Properties of Ordinary Water Substance for General and Scientific Use, J. Phys. Chem.
741 Ref. Data. 31 (2002) 387–535.
742 [39] E.W. Lemmon, M.L. Huber, Thermodynamic Properties of *n* -Dodecane, Energ.
743 Fuel. 18 (2004) 960–967.
744 [40] T. Schneider, E. Stoll, Molecular-Dynamics Study of a Three-Dimensional One-
745 Component Model for Distortive Phase Transitions, Phys. Rev. B. 17 (1978) 1302–1322.
746 [41] S. Nosé, A Molecular Dynamics Method for Simulations in the Canonical
747 Ensemble, Mol. Phys. 52 (1984) 255–268.
748 [42] H.J.C. Berendsen, J.P.M. Postma, W.F. van Gunsteren, A. DiNola, J.R. Haak,

749 Molecular Dynamics With Coupling to an External Bath, J. Chem. Phys. 81 (1998) 3684–
750 3690.

751 [43] W.G. Hoover, Constant-Pressure Equations of Motion, Phys. Rev. A. 34 (1986)
752 2499–2500.

753 [44] M.G. Martin, J.I. Siepmann, Transferable Potentials for Phase Equilibria. 1.
754 United-Atom Description of n-Alkanes, J. Phys. Chem. B. 102 (1998) 2569–2577.

755 [45] J. Wang, R.M. Wolf, J.W. Caldwell, P.A. Kollman, D.A. Case, Development and
756 Testing of a General Amber Force Field, J. Comput. Chem. 25 (2004) 1157–1174.

757 [46] W.L. Jorgensen, J. Chandrasekhar, J.D. Madura, R.W. Impey, M.L. Klein,
758 Comparison of Simple Potential Functions for Simulating Liquid Water, J. Chem. Phys.
759 79 (1983) 926–935.

760 [47] J.-P. Ryckaert, G. Ciccotti, H.J.C. Berendsen, Numerical Integration of the
761 Cartesian Equations of Motion of a System with Constraints: Molecular Dynamics of n-
762 Alkanes, J. Comput. Phys. 23 (1977) 327–341.

763 [48] H.W. Horn, W.C. Swope, J.W. Pitera, J.D. Madura, T.J. Dick, G.L. Hura, T. Head-
764 Gordon, Development of an Improved Four-Site Water Model for Biomolecular
765 Simulations: TIP4P-Ew, J. Chem. Phys. 120 (2004) 9665–9678.

766 [49] D.E. Smith, L.X. Dang, Computer Simulations of NaCl Association in Polarizable
767 Water, J. Chem. Phys. 100 (1998) 3757–3766.

768 [50] J. Åqvist, Ion-Water Interaction Potentials Derived from Free Energy Perturbation
769 Simulations, J. Phys. Chem. 94 (1990) 8021–8024.

770 [51] D. Beglov, B. Roux, Finite Representation of an Infinite Bulk System: Solvent
771 Boundary Potential for Computer Simulations, J. Chem. Phys. 100 (1998) 9050–9063.

772 [52] H.A. Lorentz, Ueber die Anwendung des Satzes vom Virial in der Kinetischen
773 Theorie der Gase, Ann. Phys. 248 (1881) 127–136.

774 [53] M. P. Allen, D. J. Tildesley, Computer Simulation of Liquids, Oxford University
775 Press, New York, 2017.

776 [54] C. Vega, E. de Miguel, Surface Tension of the Most Popular Models of Water by
777 Using the Test-Area Simulation Method, J. Chem. Phys. 126 (2007) 154707:1–10.

778 [55] C.D. Holcomb, P. Clancy, J.A. Zollweg, A critical study of the simulation of the
779 liquid-vapour interface of a Lennard-Jones fluid, Mol. Phys. 78 (1993) 437–459.

780 [56] D. Duque, L.F. Vega, Some issues on the calculation of interfacial properties by

781 molecular simulation, J. Chem. Phys. 121 (2004) 8611–8617.

782 [57] A. Ghoufi, P. Malfreyt, D.J. Tildesley, Computer modelling of the surface tension
783 of the gas–liquid and liquid–liquid interface, Chem. Soc. Rev. 45 (2016) 1387–1409.

784 [58] H. Sun, COMPASS: An ab Initio Force-Field Optimized for Condensed-Phase
785 Applications Overview with Details on Alkane and Benzene Compounds, J. Phys. Chem.
786 B. 102 (1998) 7338–7364.

787 [59] P.P. Ewald, Die Berechnung Optischer und Elektrostatischer Gitterpotentiale,
788 Ann. Phys. 369 (1921) 253–287.

789 [60] J.G. Kirkwood, F.P. Buff, The Statistical Mechanical Theory of Surface Tension,
790 J. Chem. Phys. 17 (2004) 338–343.

791 [61] J.H. Irving, J.G. Kirkwood, The Statistical Mechanical Theory of Transport
792 Processes. IV. The Equations of Hydrodynamics, J. Chem. Phys. 18 (1950) 817–829.

793 [62] W. Humphrey, A. Dalke, K. Schulten, VMD: Visual molecular dynamics, J. Mol.
794 Graph. 14 (1996) 33–38.

795 [63] R. Nagarajan, D.T. Wasan, Measurement of Dynamic Interfacial Tension by an
796 Expanding Drop Tensiometer, J. Colloid Interface Sci. 159 (1993) 164–173.

797 [64] S. Zeppieri, J. Rodríguez, A.L. López de Ramos, Interfacial Tension of Alkane +
798 Water Systems †, J. Chem. Eng. Data. 46 (2001) 1086–1088.

799 [65] R. Aveyard, S.M. Saleem, Interfacial Tensions at Alkane-Aqueous Electrolyte
800 Interfaces, J. Chem. Soc., Faraday Trans. 1. 72 (1976) 1609–1617.

801 [66] D. Bhatt, J. Newman, C.J. Radke, Molecular Dynamics Simulations of Surface
802 Tensions of Aqueous Electrolytic Solutions, J. Phys. Chem. B. 108 (2004) 9077–9084.

803 [67] E. Mayoral, E. Nahmad-Achar, Study of Interfacial Tension Between an Organic
804 Solvent and Aqueous Electrolyte Solutions Using Electrostatic Dissipative Particle
805 Dynamics Simulations, J. Chem. Phys. 137 (2012) 194701:1–10.

806 [68] P.K. Weissenborn, R.J. Pugh, Surface Tension of Aqueous Solutions of
807 Electrolytes: Relationship with Ion Hydration, Oxygen Solubility, and Bubble
808 Coalescence, J. Colloid Interface Sci. 184 (1996) 550–563.

809 [69] E.R.A. Lima, B.M. de Melo, L.T. Baptista, M.L.L. Paredes, Specific Ion Effects
810 on the Interfacial Tension of Water/Hydrocarbon Systems, Braz. J. Chem. Eng. 30 (2013)
811 55–62.

812 [70] D. Andrienko, Introduction to Liquid Crystals, J. Mol. Liq. 267 (2018) 520–541.

[71] M. Tintaru, R. Moldovan, T. Beica, S. Frunza, Surface Tension of Some Liquid Crystals in the Cyanobiphenyl Series, Liq. Cryst. 28 (2001) 793–797.

[72] D.W. Smith, Ionic Hydration Enthalpies, J. Chem. Educ. 54 (1977) 540–542.